

Probing properties of the QCD Medium using jet substructure techniques in pp and PbPb collisions at 5.02 TeV at CMS

Dhanush Anil Hangal on behalf of the CMS Collaboration*

University of Illinois at Chicago

E-mail: dhanush.anil.hangal@cern.ch

We present results on measurements of inclusive jet substructure variables using grooming techniques with pp and PbPb data collected with the CMS detector at a center-of-mass energy of 5.02 TeV per nucleon pair. Jet grooming techniques are used to focus on the hard structure of the jet by extracting the two subjets corresponding to a hard parton splitting. The resulting groomed jets can be used to study modifications to the parton shower evolution in the presence of the hot and dense medium created in heavy ion collisions. The hard jet structure is sensitive to the virtuality evolution of a parton in the medium, as well as the role of (de)coherent gluon emitters. Modifications of shared momentum fraction and jet mass over a wide range of jet transverse momentum and various collision centrality selections are reported and compared to predictions from event generators and analytical calculations.

*International Conference on Hard and Electromagnetic Probes of High-Energy Nuclear Collisions
30 September - 5 October 2018
Aix-Les-Bains, Savoie, France*

*Speaker.

1. Introduction

High-momentum partons produced during the initial hard scatterings in heavy ion collisions are predicted to suffer energy loss as they traverse the quark-gluon plasma (QGP) [1]. The mechanisms by which these partons lose energy to the medium, and their interactions with the medium, are still not fully understood [2]. The particles resulting from the fragmentation and hadronization of these partons, can be clustered into jets, and can be used as parton proxies to probe the properties of the QGP. Parton energy loss manifests itself in various experimental observables, first measured at BNL RHIC [3, 4], and subsequently at the CERN LHC [5, 6, 7], including suppression of high transverse momentum, p_T , hadrons and jets, as well as modifications of the properties of parton showers.

After an initial hard splitting, where both resulting partons carry a significant fraction of the original energy, the two energetic partons then evolve into separate sprays of particles within the jet. By isolating these two hard-radiation sources and removing the softer wide-angle radiation contributions, this initial splitting and the interactions of the color charges of the medium with the two outgoing highly energetic partons can be studied. In experiment, this is achieved using jet grooming algorithms that attempt to isolate the hard prongs of a jet and remove soft wide-angle radiation [8, 9]. Interactions of the two outgoing partons with the QCD medium could temporarily increase their virtuality leading to a different gluon emission probability, subsequently resulting in modifications of the momentum sharing and the angular separation between the split partons [10, 11].

In this work we present measurements of shared momentum fraction [12] and groomed jet mass [13]. Shared momentum fraction, z_g , is defined as the ratio between the p_T of the less energetic subjet, $p_{T,2}$, and the p_T sum of the two subjets [14], $z_g = p_{T,2}/(p_{T,1} + p_{T,2})$. In pp collisions, the variable z_g corresponds to the QCD splitting function and is independent of the jet p_T [15]. In PbPb collisions, this measurement helps to probe the role of color coherence of the jet in the medium, including the ability of the medium to resolve the partons by breaking the color coherence between them [16]. If the partons act as a single coherent emitter, the two subjets will be equally modified, leaving z_g unaffected [17]. If, instead, the partons in the medium act as decoherent emitters, the two subjets should be modified differently, thereby altering z_g . The ability of the medium to resolve the traversing partons also depends on the opening angle of their splitting [18, 19], which motivates studies of the groomed jet mass (M_g). Jet mass is defined as the invariant mass of the system consisting of two subjets, and is sensitive to both the parton splitting function and the opening angle between the two outgoing partons. The variable used in the groomed jet mass measurements is M_g/p_T^{jet} as the invariant jet mass scales with jet p_T in vacuum [21] leading to partial cancellation in systematic uncertainties. In addition, both z_g and M_g/p_T^{jet} are sensitive to semi-hard medium-induced gluon radiation [18], modifications of the initial parton splitting [19], and the medium response [20].

2. Analysis and Results

Data samples of PbPb and pp data at $\sqrt{s_{\text{NN}}} = 5.02$ TeV, corresponding to integrated luminosities of $404 \mu\text{b}^{-1}$ and 25pb^{-1} , respectively, were used in these measurements. Events are selected

using high p_T jet triggers. In pp collisions, an unprescaled trigger with a jet p_T threshold of $p_T^{\text{jet}} = 80$ GeV is used, based on jets reconstructed from particle-flow candidates [22]. In PbPb collisions, triggers are based on jets reconstructed from calorimeter deposits including a subtraction of the uncorrelated underlying event. The threshold for these triggers is $p_T^{\text{jet}} = 100$ GeV. The anti- k_T algorithm [23] with the distance parameter $R = 0.4$ is used for these measurements in both pp and PbPb collisions.

In order to remove contributions from the underlying event activity, the ‘‘constituent subtraction’’ [24] algorithm is performed for each jet. The algorithm takes the per-event background energy density as input and performs a particle-based background subtraction. The average event activity is estimated following methods described in Ref. [25]. To compare results from pp collisions with those of PbPb collisions in a given p_T^{jet} and centrality range, a smearing procedure is applied to the pp data in order to account for the effects of the presence of underlying event activity and differences in the reconstruction procedure between PbPb and pp data. The corrections for the smearing procedure are derived by comparing fully simulated and reconstructed PYTHIA [26] events with PYTHIA events embedded in HYDJET [27] background.

Jet grooming algorithms [8, 9, 21] are used to remove the contributions from large angle soft radiation of the jet and underlying event activities, and to focus on the hard structure of the jet. In the soft drop (SD) algorithm [9, 14] that is adopted here, a reconstructed jet (using the anti- k_T algorithm) is first re-clustered using the Cambridge-Aachen algorithm [28] and then de-clustered by dropping the softer branch until finding two hard branches with the following condition satisfied:

$$z_g = \frac{\min(p_{T,1}, p_{T,2})}{p_{T,1} + p_{T,2}} > z_{\text{cut}} \left(\frac{\Delta R_{12}}{R_0} \right)^\beta \quad (2.1)$$

where $p_{T,1}$ ($p_{T,2}$) denote the transverse momentum of the first (second) subjet, and θ is the angular separation between the two subjets. z_{cut} and β are free parameters we can choose for different types of jet grooming. The algorithm terminates if the soft drop condition is met, failing which, the smaller of the two subjets is discarded and the two subjets of the leading subjet are examined. In these measurements, two sets of parameters are considered: $z_{\text{cut}} = 0.1$ with $\beta = 0.0$, denoted as (0.1, 0.0) SD setting, and $z_{\text{cut}} = 0.5$ with $\beta = 1.5$, denoted as (0.5, 1.5) SD setting. The first parameter set has the advantage of being largely insensitive to higher-order QCD corrections, such as multiple emissions, while the second one is preferred experimentally since it reduces the impact from underlying event fluctuations by applying a stronger SD constraint for subjets with larger opening angle, thereby focusing on the core of the jet. An additional cut of $\Delta R_{12} > 0.1$ is applied to account for detector (in)efficiency and to avoid the collinear region.

The per jet normalized z_g and M_g/p_T^{jet} distributions in pp collisions are presented in Fig. 1, left and right panels respectively, for p_T^{jet} between 160 and 180 GeV for different SD settings. It is observed that the results from the Monte Carlo (MC) generators and data agree within systematic uncertainties for both measurements. The z_g distribution for pp collisions follows the characteristic $1/z$ behavior expected from the QCD splitting function [15]. It is also noted that the M_g/p_T^{jet} measurements, which are sensitive to large angle soft radiation, are considerably different in the two grooming settings.

Fig. 2 (left panel) shows the z_g distribution measured in PbPb collisions for p_T^{jet} between 160 and 180 GeV, in different centrality intervals, in comparison to the smeared pp reference data. It

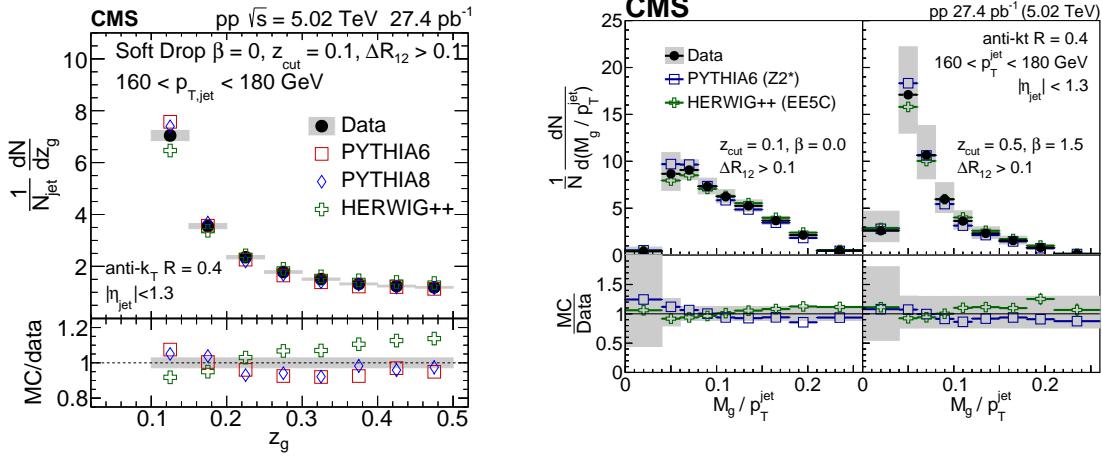


Figure 1: Left: The z_g distribution in pp collisions in the (0.1,0.0) SD setting compared to predictions from event generators. Right: The M_g/p_T^{jet} distribution for pp collisions using (0.1,0.0) SD setting (left panels) and (0.5, 1.5) SD setting (right panels). Results are shown for $160 < p_T^{\text{jet}} < 180$ GeV and compared to PYTHIA and HERWIG++ event generators in both measurements. The shaded area indicate systematic uncertainties and the statistical uncertainties are less than the marker sizes. For more details please refer to Ref. [12] and Ref. [13].

is observed that the z_g distribution in peripheral PbPb collisions is in agreement with the the pp measurement and that as the PbPb collisions become more central the splitting into two branches becomes increasingly more unbalanced. The modification of the z_g distribution in central PbPb collisions is shown in Fig. 2 (right panel) for various kinematic ranges in p_T^{jet} . The results are compared to a prediction from the JEWEL event generator which incorporates medium-induced interactions while the partons propagate through the QGP [20, 32], and also to predictions from various theoretical models [19, 29, 30] with different settings.

Fig. 3 and Fig. 4 show the M_g/p_T^{jet} distributions measured in PbPb collisions for the two grooming settings, in different centrality intervals, in comparison to the smeared pp reference data for p_T^{jet} between 160 and 180 GeV. No significant modification in PbPb collisions compared to smeared pp data is observed for the (0.1,0.0) SD setting, except for a hint of an enhancement of large mass jets for the 10% most central collisions. For the (0.5, 1.5) SD setting, where the grooming is more likely to remove pairs of subjets with large opening angles or highly imbalanced p_T values, no noticeable modification is observed.

The ratio of M_g/p_T^{jet} distributions in the 0 – 10% PbPb collisions sample to that in pp smeared sample are shown for several p_T^{jet} intervals in Fig. 5, for the two grooming settings. The results are compared to two jet quenching event generators which incorporate medium-induced radiation in the parton splitting process, i.e., JEWEL (with and without the recoil setting) and Q-PYTHIA [31]. It is observed that of the models compared to data here, none describe the jet mass measurements for the two grooming settings simultaneously.

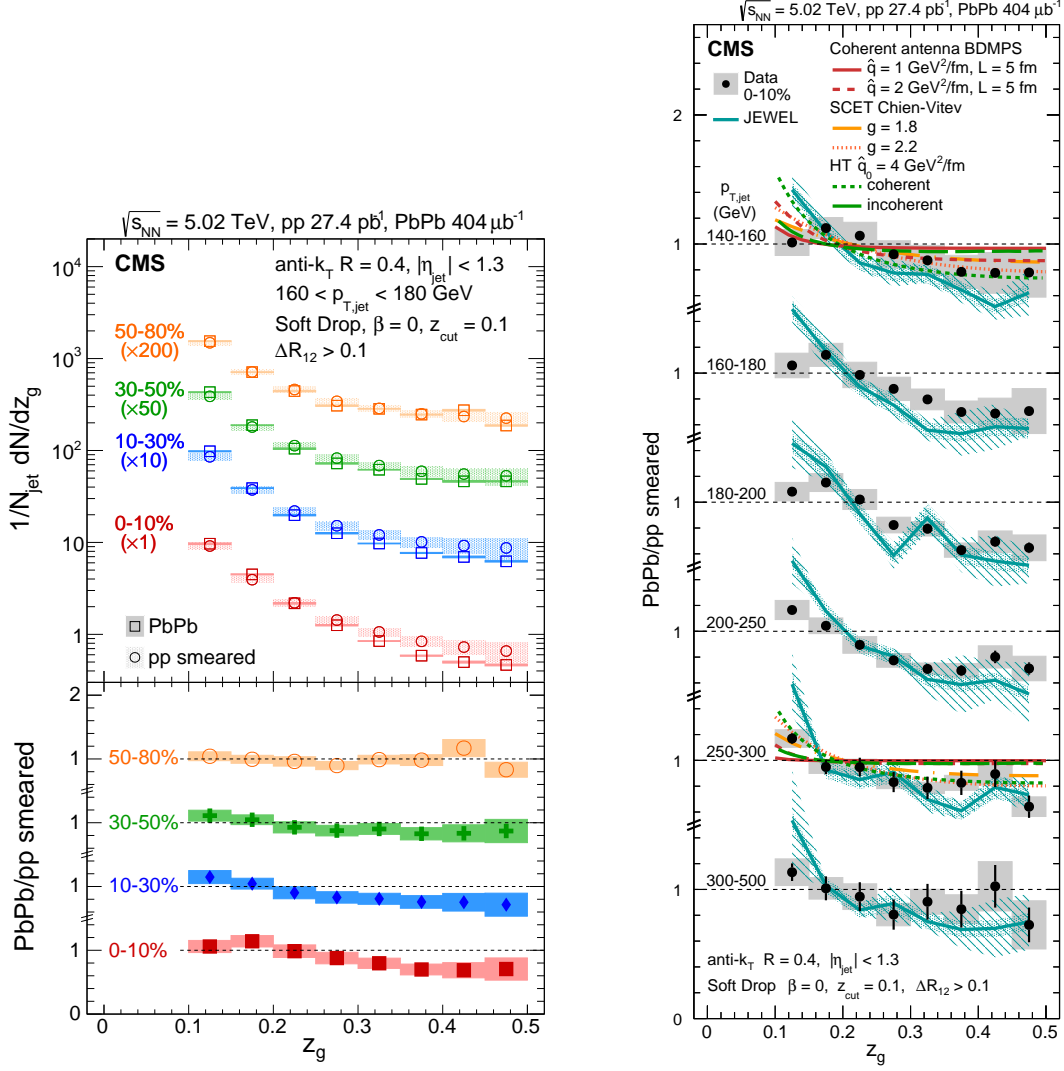


Figure 2: Left: The z_g distributions in PbPb collisions for $160 < p_T^{\text{jet}} < 180$ GeV, in several centrality ranges, compared to pp data smeared to account for the differences in resolution. The error bars (shaded area) represent the statistical (systematic) uncertainty. Right: Ratios of z_g distributions in the 10% most central PbPb collisions to that in the smeared pp collisions, for several p_T^{jet} ranges, compared to various jet quenching theoretical calculations [19, 29, 30]. The error bars (shaded area) represent the statistical (systematic) uncertainty. The diagonally hatched band denotes the uncertainty from the treatment of the medium response using the JEWEL event generator. For more details please refer to Ref. [12].

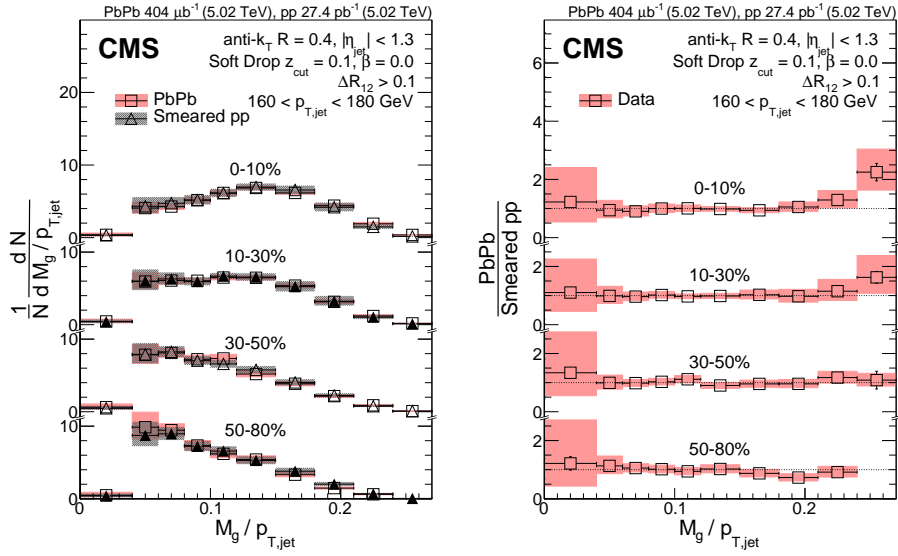


Figure 3: Left: The centrality dependence of M_g/p_T^{jet} , for PbPb events with $160 < p_T^{\text{jet}} < 180$ GeV for the (0.1,0.0) SD setting. Results are compared to the smeared pp spectra. Right: The ratio of PbPb data over smeared pp data. The heights of the vertical lines (colored boxes) indicate statistical (systematic) uncertainties. Statistical uncertainties are less than the marker sizes in most bins. For more details please refer to Ref. [13].

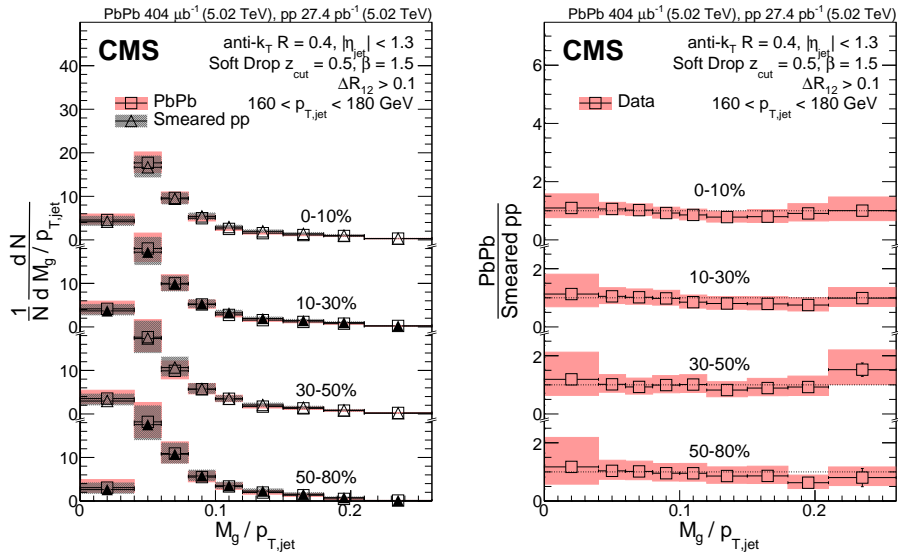


Figure 4: Left: The centrality dependence of M_g/p_T^{jet} , for PbPb events with $160 < p_T^{\text{jet}} < 180$ GeV for the (0.5,1.5) SD setting. Results are compared to the smeared pp spectra. Right: The ratio of PbPb data over smeared pp data. The heights of the vertical lines (colored boxes) indicate statistical (systematic) uncertainties. Statistical uncertainties are less than the marker sizes in most bins. For more details please refer to Ref. [13].

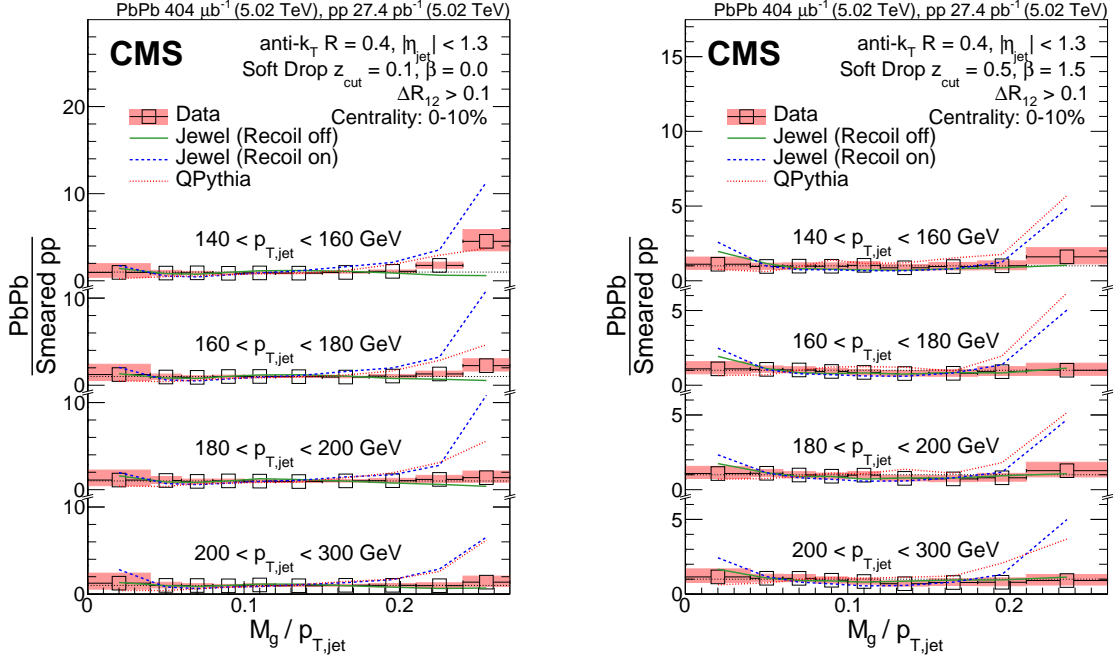


Figure 5: Ratios of M_g/p_T^{jet} distributions in the 10% most central PbPb collisions to that in the smeared pp collisions for the (0.1, 0.0) SD setting (left) and (0.5, 1.5) SD setting (right), in several p_T^{jet} ranges. The heights of the colored boxes indicate systematic uncertainties. Statistical uncertainties are less than the marker sizes. The ratios are compared to smeared JEWEL and Q-PYTHIA generators, shown in blue and green, respectively. For more details please refer to Ref. [13].

3. Summary

Measurements of the shared momentum fraction (z_g) and the groomed jet mass (M_g/p_T^{jet}) are reported using pp and PbPb collisions at $\sqrt{s_{\text{NN}}} = 5.02$ TeV collected by the CMS experiment. Using the ($z_{\text{cut}} = 0.1, \beta = 0.0$) SD grooming setting for which the grooming is independent of the angular separation of the subjets, we observe an agreement in the z_g distribution between peripheral PbPb and pp collisions and as the PbPb collisions become more central, a steepening of the spectrum is observed, implying a more unbalanced splitting. Additionally, no significant modification of the M_g/p_T^{jet} spectra is observed in the 10-80% peripheral PbPb collisions with respect to the measurement in pp collisions. However, for the 10% most central collisions, a hint of increased probability to produce jets with large M_g/p_T^{jet} is seen when compared to pp collisions for jets with $140 < p_T^{\text{jet}} < 180$ GeV. For the SD grooming setting that remove more radiation at distances far away from the jet axis ($z_{\text{cut}} = 0.5, \beta = 1.5$), the M_g/p_T^{jet} distribution in PbPb collisions is in agreement within uncertainties with that measured in pp collisions for all studied centrality (0-80%) and p_T^{jet} (140-300 GeV) regions.

References

- [1] J. D. Bjorken, *Energy loss of energetic partons in QGP: possible extinction of high p_T jets in hadron-hadron collisions*, (1982). FERMILAB-PUB-82-059-THY.
- [2] G-Y Qin and X-N Wang, *Jet quenching in high-energy heavy-ion collisions*, *Int.J.Mod.Phys. E24* (2015) no.11, 1530014 [hep-ph/1511.00790]
- [3] STAR Collaboration, *Direct observation of dijets in central Au+Au collisions at $\sqrt{s_{NN}} = 200$ GeV*, *Phys. Rev. Lett.* 97 (2006) 162301, [nucl-ex/0604018].
- [4] PHENIX Collaboration, *Transverse momentum and centrality dependence of dihadron correlations in Au+Au collisions at $\sqrt{s_{NN}} = 200$ GeV: Jet-quenching and the response of partonic matter*, *Phys. Rev. C* 77 (2008) 011901, arXiv:0705.3238.
- [5] ATLAS Collaboration, *Observation of a centrality-dependent dijet asymmetry in lead-lead collisions at $\sqrt{s_{NN}} = 2.76$ TeV with the ATLAS detector at the LHC*, *Phys. Rev. Lett.* 105 (2010) 252303, arXiv:1011.6182.
- [6] CMS Collaboration, *Observation and studies of jet quenching in PbPb collisions at $\sqrt{s_{NN}} = 2.76$ TeV*, *Phys. Rev. C* 84 (2011) 024906, arXiv:1102.1957.
- [7] ALICE Collaboration, *Measurement of jet suppression in central Pb-Pb collisions at $\sqrt{s_{NN}} = 2.76$ TeV*, *Phys. Lett. B* 746 (2015) 1, arXiv:1502.01689
- [8] J. M. Butterworth, A. R. Davison, M. Rubin & G. P. Salam, *Jet substructure as a new Higgs search channel at the LHC*, *Phys. Rev. Lett.* 100 (2008) 242001, arXiv:0802.2470.
- [9] A. J. Larkoski, S. Marzani, G. Soyez, & J. Thaler, *Soft drop*, *JHEP* 05 (2014) 146, arXiv:1402.2657.
- [10] I. Vitev, *Large angle hadron correlations from medium-induced gluon radiation*, *Phys.Lett.B* 630 (2005) 78–84, arXiv:hep-ph/0501255.
- [11] T. Renk, *YaJEM: a Monte Carlo code for in-medium shower evolution*, *Int.J.Mod.Phys.E* 20 (2011) 1594–1599. arXiv:1009.3740, doi:10.1142/S0218301311019933.
- [12] CMS Collaboration, *Measurement of the splitting function in pp and PbPb collisions at $\sqrt{s_{NN}} = 5.02$ TeV*, *Phys. Rev. Lett.* 120 (2018) 142302, doi:10.1103/PhysRevLett.120.142302, arXiv:1708.09429.
- [13] CMS collaboration, *Measurement of the groomed jet mass in PbPb and pp collisions at $\sqrt{s_{NN}} = 5.02$ TeV* *J. High Energ. Phys.* (2018) 2018: 161. doi:10.1007/JHEP10(2018)161, arXiv:1805.05145
- [14] A. J. Larkoski, S. Marzani, & J. Thaler, *Sudakov Safety in Perturbative QCD*, *Phys. Rev. D* 91 (2015) 111501, doi:10.1103/PhysRevD.91.111501, arXiv:1502.01719.
- [15] A. Larkoski et al., *Exposing the QCD splitting function with CMS Open Data*, *Phys. Rev. Lett.* 119 (2017) 132003, doi:10.1103/PhysRevLett.119.132003, arXiv:1704.05066.
- [16] Y. Mehtar-Tani & K. Tywoniuk, *Jet (de)coherence in Pb–Pb collisions at the LHC*, *Phys. Lett. B* 744 (2015) 284, doi:10.1016/j.physletb.2015.03.041, arXiv:1401.8293.
- [17] J. Casalderrey-Solana, Y. Mehtar-Tani, C. A. Salgado, & K. Tywoniuk, *New picture of jet quenching dictated by color coherence*, *Phys. Lett. B* 725 (2013) 357, doi:10.1016/j.physletb.2013.07.046, arXiv:1210.7765.
- [18] Y. Mehtar-Tani & K. Tywoniuk, *Groomed jets in heavy-ion collisions: sensitivity to medium-induced bremsstrahlung*, *JHEP* 04 (2017) 125, doi:10.1007/JHEP04(2017)125, arXiv:1610.08930.

- [19] Y.-T. Chien & I. Vitev, *Probing the Hardest Branching within Jets in Heavy-Ion Collisions*, *Phys. Rev. Lett.* 119 (2017) 112301, doi:10.1103/PhysRevLett.119.112301, arXiv:1608.07283.
- [20] G. Milhano, U. A. Wiedemann, & K. C. Zapp, *Sensitivity of jet substructure to jet-induced medium response*, (2017). arXiv:1707.04142.
- [21] M. Dasgupta, A. Fregoso, S. Marzani, & G. P. Salam, *Towards an understanding of jet substructure*, *JHEP* 9 (2013) 29, doi:10.1007/JHEP09(2013)029, arXiv:1307.0007.
- [22] CMS Collaboration, *Commissioning of the Particle-Flow event reconstruction with the first LHC collisions recorded in the CMS detector*, CMS Physics Analysis Summary CMS-PAS-PFT-10-001 (2010).
- [23] M. Cacciari, G. P. Salam, G. Soyez, *Fastjet user manual* arXiv:1111.6097
- [24] P. Berta, M. Spusta, D. W. Miller, R. Leitner, *Particle-level pileup subtraction for jets and jet shapes*, *JHEP* 1406 (2014) 092. arXiv:1403.3108, doi:10.1007/JHEP06(2014)092.
- [25] G. Soyez, G. P. Salam, J. Kim, S. Dutta, M. Cacciari, *Pileup subtraction for jet shapes*, *Phys.Rev.Lett.* 110 (16) (2013) 162001. arXiv:1211.2811, doi:10.1103/PhysRevLett.110.162001.
- [26] T. Sjostrand, S. Mrenna, P. Skands, *PYTHIA 6.4 physics and manual*, *JHEP* 05 (2006) 026. arXiv:hep-ph/0603175, doi:10.1088/1126-6708/2006/05/026.
- [27] I. P. Lokhtin, A. M. Snigirev, *A model of jet quenching in ultrarelativistic heavy ion collisions and high-pt hadron spectra at RHIC*, *The European Physical Journal C - Particles and Fields* 45 (1) (2006) 211-217. doi:10.1140/epjc/s2005-02426-3.
- [28] Y. L. Dokshitzer, G. D. Leder, S. Moretti, B. R. Webber, *Better jet clustering algorithms*, *JHEP* 08 (1997) 001. arXiv:hep-ph/9707323, doi:10.1088/1126-6708/1997/08/001.
- [29] R. Baier et al., *Radiative energy loss of high-energy quarks and gluons in a finite volume quark-gluon plasma*, *Nucl. Phys. B* 483 (1997) 291, doi:10.1016/S0550-3213(96)00553-6, arXiv:hep-ph/9607355.
- [30] N.-B. Chang, S. Cao, and G.-Y. Qin, *Probing medium-induced jet splitting and energy loss in heavy-ion collisions*, (2017). arXiv:1707.03767.
- [31] N. Armesto, L. Cunqueiro, and C. A. Salgado, *Q-PYTHIA: A medium-modified implementation of final state radiation*, *Eur. Phys. J. C* 63 (2009) 679, doi:10.1140/epjc/s10052-009-1133-9, arXiv:0907.1014.
- [32] R. Kunnawalkam Elayavalli and K. C. Zapp, *Medium response in JEWEL and its impact on jet shape observables in heavy ion collisions*, *JHEP* 07 (2017) 141, doi:10.1007/JHEP07(2017)141, arXiv:1707.01539.